


 Cite this: *RSC Adv.*, 2022, **12**, 25118

 Received 11th July 2022
 Accepted 29th August 2022

 DOI: 10.1039/d2ra04270c
rsc.li/rsc-advances

Insight into systematic formation of hexafluorosilicate during crystallization *via* self-assembly in a glass vessel†

 Dongwon Kim, ^a Jihun Han, ^a Ok-Sang Jung, ^{*a} and Young-A. Lee ^{*b}

Formation of the unexpected hexafluorosilicate (SiF_6^{2-}) anion during crystallization *via* self-assembly in glassware is scrutinized. Self-assembly of $\text{M}(\text{BF}_4)_2$ ($\text{M}^{2+} = \text{Cu}^{2+}$ and Zn^{2+}) with tridentate N-donors (L) in a mixture solvent including methanol in a glass vessel gives rise to an SiF_6^{2-} -encapsulated Cu_3L_4 double-decker cage and a Zn_2L_4 cage, respectively. Induced reaction of CuX_2 ($\text{X}^- = \text{PF}_6^-$ and SbF_6^-) instead of $\text{Cu}(\text{BF}_4)_2$, with the tridentate ligands, produces the same species. The formation time of SiF_6^{2-} is in the order of anions $\text{BF}_4^- < \text{PF}_6^- < \text{SbF}_6^-$ under the given reaction conditions. The SiF_6^{2-} anion, acting as a cage template or cage-to-cage bridge, seems to be formed from the reaction of polyatomic anions containing fluoride with the SiO_2 of the surface of the glass vessel.

Introduction

Anion-related chemistry is a rapidly burgeoning field owing to the timeliness and importance including environmental pollution, industrial chemicals, biological processes, ionic liquids, lithium batteries, templates, ion-pairing, and health.^{1–12} Some anions play a significant role in the construction and behaviors of desirable molecular architectures based on negative charge, size, shape, solvents, and pH.^{13–18} In particular, F-containing polyatomic anions such as BF_4^- , PF_6^- , and SbF_6^- have been extensively employed for various purposes such as important chemical phenomena, cage-templates, coordination, and the Hofmeister series;^{19–26} however, they are known to be not thermodynamically stable depending on conditions^{27,28} relative to the F-free polyatomic anions NO_3^- , ClO_4^- , CH_3CO_2^- , and SO_4^{2-} . For instance, the PF_6^- anion could be converted to $\text{PF}_n(\text{OH})_{6-n}^-$ during the complexation of $\text{Pd}(\text{II})\text{-L}$.²⁹ Furthermore, BF_4^- is known to be changed to the SiF_6^{2-} anion *via* subsequent reaction of dissociated F^- with the Si–O moieties of a glass vessel or stoneware.^{30–35} Hexafluorosilicate (SiF_6^{2-}) is a stable octahedral anion with six Si–F bond distances of 1.71 Å,³⁶ and its solubility is significantly dependent on cations.³⁷ Furthermore, the dianion species have seen the following diverse uses: leather and wood preservation agents, fluoridation agents for drinking water, two-solution

fluoride mouth rinse, commercial laundry, enamels/enamel frits for china and porcelain, opalescent glass, metallurgy of aluminum and beryllium, glue, ore flotation, insecticides and rodenticides, fluorinating agent in organic synthesis, and water fluoridation.^{38–47}

In this context, systematic research on the unusual formation process and recognition of SiF_6^{2-} is very much in demand. Thus, herein, formation of hexafluorosilicate *via* conversion of PF_6^- and SbF_6^- beside BF_4^- during self-assembly or recrystallization in a glass vessel is scrutinized. This paper reports the unique SiF_6^{2-} -encapsulated cages constructed *via* self-assembly of M^{2+} ($\text{M} = \text{Cu}^{2+}$ and Zn^{2+}) with tridentate N-donor ligands in a glass vessel. To our knowledge, this article presents clear systematic research on the formation of hexafluorosilicate by reactions of glassware with F-containing polyatomic anions.

Experimental

Materials and measurements

All of the chemicals, including copper(II) tetrafluoroborate ($\text{Cu}(\text{BF}_4)_2$), copper(II) nitrate ($\text{Cu}(\text{NO}_3)_2$), copper(II) chloride (CuCl_2), silver(I) hexafluorophosphate (AgPF_6), silver(I) hexafluoroantimonate (AgSbF_6), and zinc(II) tetrafluoroborate ($\text{Zn}(\text{BF}_4)_2$), were purchased from Aldrich and used without further purification. $(1S,1'S,1''S,2R,2'R,2''R)$ -(Benzenetricarbonyltris(azanediyl))tris(2,3-dihydro-1H-indene-2,1-diyl)tris(isonicotinate) (L^1) and 1,3,5-tris(isonicotinoyloxy-methyl)benzene (L^2) were synthesized according to the literature,^{48,49} respectively. Glass vessels (Hubena Co, Seongnam, Korea) were employed in all of the self-assembly reactions. The ¹H and ¹⁹F NMR spectra were recorded on a Varian Mercury Plus operating at 400 MHz. The infrared (IR) spectra were obtained on a Nicolet 380 FT-IR spectrophotometer with samples prepared as

^aDepartment of Chemistry, Pusan National University, Busan 46241, Republic of Korea. E-mail: oksjung@pusan.ac.kr; Fax: (+82) 51-5163522; Tel: (+82) 51-5103240

^bDepartment of Chemistry, Jeonbuk National University, Jeonju 54896, Korea. E-mail: ylee@jbnu.ac.kr

† Electronic supplementary information (ESI) available. CCDC 2180982 and 2180983. For ESI and crystallographic data in CIF or other electronic format see <https://doi.org/10.1039/d2ra04270c>



KBr pellets. Elemental microanalyses (C, H, N) were performed on solid samples at the Pusan Center, KBSI, using a Vario-EL III. Thermal analyses were carried out under a dinitrogen atmosphere at a scan rate of $10^{\circ}\text{C min}^{-1}$ using a Labsys TGA-DSC 1600.

$[(\text{SiF}_6)_2@\text{Cu}_3\text{L}^1_4](\text{SiF}_6)\cdot 16\text{CH}_3\text{OH}$

Method 1. A methanol solution (2.0 mL) of copper(II) tetrafluoroborate (4.7 mg, 0.02 mmol) was carefully layered onto a dichloromethane solution (2.0 mL) of L^1 (18.4 mg, 0.02 mmol). After 2 weeks, blue crystals suitable for single crystal X-ray structure determination were obtained in an 83% yield.

Method 2. A methanol solution (1.0 mL) of silver(I) hexafluorophosphate (10.1 mg, 0.04 mmol) was added to copper(II) chloride (2.7 mg, 0.02 mmol) dispersed in methanol at room temperature. The reaction mixture was stirred for 30 min, after which, the precipitated silver chloride was filtered off. The methanol solution of $\text{Cu}(\text{PF}_6)_2$ was carefully layered onto a dichloromethane solution (2.0 mL) of L^1 (18.4 mg, 0.02 mmol). After 4 weeks, blue crystals suitable for single crystal X-ray structure determination were obtained in a 78% yield.

Method 3. A methanol solution (1.0 mL) of silver(I) hexafluoroantimonate (13.7 mg, 0.04 mmol) was added to a suspension of copper(II) chloride (2.7 mg, 0.02 mmol) dispersed in methanol at room temperature. The reaction mixture was stirred for 30 min, after which, the precipitated silver chloride was filtered off. The methanol solution of $\text{Cu}(\text{SbF}_6)_2$ was carefully layered onto a dichloromethane solution (2.0 mL) of L^1 (18.4 mg, 0.02 mmol). After 6 weeks, blue crystals suitable for single crystal X-ray structure determination were obtained in a 66% yield.

Method 4. A methanol solution (2.0 mL) of copper(II) nitrate (2.8 mg, 0.015 mmol), a dichloromethane solution (4.0 mL) of L^1 (18.4 mg, 0.02 mmol), and an aqueous solution (0.1 mL) of $(\text{NH}_4)_2\text{SiF}_6$ (3.6 mg, 0.02 mmol) were left at room temperature, and after 1 day, blue crystals suitable for single crystal X-ray structure determination were obtained in a 62% yield. m. p. 280°C (dec). Anal. Calcd for: C, 58.55; H, 4.65; N, 7.19%. Found: C, 58.40; H, 4.52; N, 7.23%. IR (KBr pellet, cm^{-1}): 3294(br), 1733(s), 1661(s), 1524(s), 1425(m), 1329(m), 1286(s), 1179(w), 1127(s), 1063(m), 1032(m), 859(w), 756(s), 705(s), 472(w).

$[(\text{SiF}_6)_2@\text{Zn}_2\text{L}^2_4](\text{SiF}_6)\cdot 2\text{C}_4\text{H}_8\text{O}\cdot 4\text{CH}_2\text{Cl}_2$

A mixture of tetrahydrofuran with a methanol solution (3.0 mL/1.0 mL) of zinc(II) tetrafluoroborate (9.6 mg, 0.04 mmol) and a dichloromethane solution (3.0 mL) of L^2 (14.5 mg, 0.04 mmol) were left at room temperature, and after 2 weeks, blue crystals suitable for single crystal X-ray structure determination were obtained in a 67% yield. m. p. 260°C (dec). Anal. Calcd for: C, 50.88; H, 3.84; N, 5.93%. Found: C, 50.79; H, 3.81; N, 5.97%. IR (KBr pellet, cm^{-1}): 3425(br), 1729(s), 1616(w), 1564(w) 1409(m), 1373(w) 1326(m), 1280(s), 1224(w), 1122(s), 1062(m), 1024(w), 862(m), 759(s), 705(s), 468(w).

Single crystal X-ray structure determination

The X-ray diffraction data for $[(\text{SiF}_6)_2@\text{Cu}_3\text{L}^1_4](\text{SiF}_6)\cdot 16\text{CH}_3\text{OH}$ were measured at 100 K with synchrotron radiation ($\lambda = 0.76000$

Table 1 Selected bond lengths (Å) and angles (°) for $[(\text{SiF}_6)_2@\text{Cu}_3\text{L}^1_4](\text{SiF}_6)\cdot 16\text{CH}_3\text{OH}$, and $[(\text{SiF}_6)_2@\text{Zn}_2\text{L}^2_4](\text{SiF}_6)\cdot 2\text{C}_4\text{H}_8\text{O}\cdot 4\text{CH}_2\text{Cl}_2$

$[(\text{SiF}_6)_2@\text{Cu}_3\text{L}^1_4](\text{SiF}_6)\cdot 16\text{CH}_3\text{OH}$	$[(\text{SiF}_6)_2@\text{Zn}_2\text{L}^2_4](\text{SiF}_6)\cdot 2\text{C}_4\text{H}_8\text{O}\cdot 4\text{CH}_2\text{Cl}_2$		
Cu(1)-N(6)	2.007(4)	Zn(1)-N(1)	2.115(4)
Cu(1)-N(3)	2.019(3)	Zn(1)-F(4)	2.122(5)
Cu(1)-F(5)	2.317(2)	Zn(1)-F(3)	2.361(5)
N(6) ^a -Cu(1)-N(6)	87.5(2)	N(1)-Zn(1)-N(1) ^a	89.952(6)
N(6) ^a -Cu(1)-N(3) ^a	176.4(3)	N(1) ^a -Zn(1)-N(1) ^b	176.7(2)
N(6)-Cu(1)-N(3) ^a	91.2(2)	N(1) ^a -Zn(1)-N(1) ^c	89.953(6)
N(6)-Cu(1)-N(3)	176.4(2)	N(1)-Zn(1)-F(4)	91.6(1)
N(3) ^a -Cu(1)-N(3)	90.3(3)	N(1)-Zn(1)-F(3)	88.4(1)
		F(4)-Zn(1)-F(3)	180.0

^a $x - 1, y + 1, z, x + 1, y - 1, z$. ^b $x + 1, y, z - 1$. ^c $-x + 1/2, -y + 1/2, z$

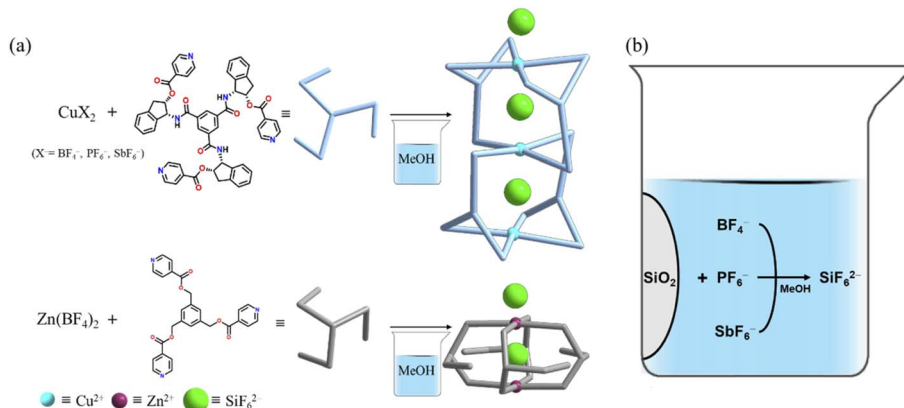
Å) on a Rayonix MX225HS detector at 2D SMC with a silicon (111) double-crystal monochromator (DCM) at the Pohang Accelerator Laboratory (PAL), Korea. The PAL BL2D-SMDC program⁵⁰ was used for data collection (detector distance: 66 mm, omega scan: $\Delta\omega = 3^{\circ}$, exposure time: 1 s per frame), and HKL3000sm (ver. 703r)⁵¹ was used for cell refinement, reduction, and absorption correction. X-ray data on $[(\text{SiF}_6)_2@\text{Zn}_2\text{L}^2_4](\text{SiF}_6)\cdot 2\text{C}_4\text{H}_8\text{O}\cdot 4\text{CH}_2\text{Cl}_2$ were collected on a Bruker SMART automatic diffractometer with graphite-monochromated Mo $\text{K}\alpha$ radiation ($\lambda = 0.71073$ Å). Thirty-six (36) frames of 2D diffraction images were collected and processed to obtain the cell parameters and orientation matrix. The data were corrected for Lorentz and polarization effects. The absorption effects were corrected using the multi-scan method (SADABS).⁵² The structures were resolved using the direct method (SHELXS) and refined by full-matrix least squares techniques (SHELXL 2018/3).⁵³ The non-hydrogen atoms were refined anisotropically, and the hydrogen atoms were placed in calculated positions and refined only for the isotropic thermal factors. The crystal parameters and procedural information corresponding to the data collection and structure refinement are listed in Table 1.

Results and discussion

Synthesis aspects

Self-assembly of $\text{Cu}(\text{BF}_4)_2$ with L^1 in a mixture of methanol and dichloromethane produced crystals consisting of $[(\text{SiF}_6)_2@\text{Cu}_3\text{L}^1_4](\text{SiF}_6)\cdot 16\text{CH}_3\text{OH}$ suitable for single crystal X-ray structure determination after 2 weeks, as shown in Scheme 1. Moreover, the reactions with $\text{Cu}(\text{PF}_6)_2$ and $\text{Cu}(\text{SbF}_6)_2$ instead of $\text{Cu}(\text{BF}_4)_2$ gave rise to the same product after significant durations, specifically 4 and 6 weeks, respectively. The reaction time may be owed to the stability of the $\text{BF}_4^- < \text{PF}_6^- < \text{SbF}_6^-$ anions under the given reaction conditions. As expected, self-assembly of $\text{Cu}(\text{BF}_4)_2$ with L^1 in the presence of $(\text{NH}_4)_2\text{SiF}_6$ produced blue crystals within 1 day. In order to investigate the metal effects, self-assembly of $\text{Zn}(\text{BF}_4)_2$ instead of $\text{Cu}(\text{BF}_4)_2$ with L^2 was performed, which generated crystals of $[(\text{SiF}_6)_2@\text{Zn}_2\text{L}^2_4](\text{SiF}_6)\cdot 2\text{C}_4\text{H}_8\text{O}\cdot 4\text{CH}_2\text{Cl}_2$ after 2 weeks, indicating that the central metal cation is not a significant factor in anion transformation in a glass vessel. For all of the reactions, the SiF_6^{2-} anion acted





Scheme 1 Construction of cages (a) via SiF_6^{2-} formation (b) during self-assembly in a glass vessel.

either as a template by which to form the cage products or as a cage-to-cage bridge.

Both crystalline products are stable under anaerobic condition at room temperature. The crystals are insoluble in common organic solvents such as acetone, chloroform, toluene, benzene and tetrahydrofuran, but are partially dissociated in dimethyl sulfoxide and *N,N*-dimethylformamide. Their compositions and structures were confirmed by elemental analyses, IR-spectral analysis (Fig. S1 and S2†), thermal analysis (Fig. S3†), ^1H NMR (Fig. S4, as dissoociated in $\text{Me}_2\text{SO}-d_6$ †), and single-crystal X-ray crystallography. The characteristic IR bands of SiF_6^{2-} were easily assigned. The thermogravimetric analysis (TGA) and differential scanning calorimetry (DSC) showed $[(\text{SiF}_6)_2@\text{Cu}_3\text{L}^1_4](\text{SiF}_6) \cdot 16\text{CH}_3\text{OH}$ and $[(\text{SiF}_6)@\text{Zn}_2\text{L}^2_4](\text{SiF}_6) \cdot 2\text{C}_4\text{H}_8\text{O} \cdot 4\text{CH}_2\text{Cl}_2$ to be stable up to 277 and 257 °C, respectively. Evaporation of the solvate molecules of the two kinds of crystals occurred in the 10–60 and 20–135 °C temperature ranges, respectively (Fig. S3†).

Crystal structures

The crystal structure of $[(\text{SiF}_6)_2@\text{Cu}_3\text{L}^1_4](\text{SiF}_6) \cdot 16\text{CH}_3\text{OH}$ is depicted in Fig. 1, and its bond lengths and angles are listed in Table 1. The geometry of each copper(II) ion is an octahedral N_4F_2 coordination arrangement with four N donors from four L^1 's and F donors from two SiF_6^{2-} anions ($\text{Cu}-\text{N} = 2.007(4) - 2.019(3)$ Å; $\text{Cu}-\text{F}(\text{encapsulated}) = 2.317(2)$, 2.300(3) Å; $\text{Cu}-\text{F}(\text{bridged}) = 2.357(3)$ Å) in axial positions, resulting in the formation of the Cu_3L_4 double-decker occupied by two SiF_6^{2-} anions. Concomitantly, for the nested SiF_6^{2-} , the equatorial Si–F bond lengths ($1.628(7) - 1.684(7)$ Å) are comparable to the axial Si–F lengths (1.666(3) and 1.693(3) Å). Thus, the ligand is coordinated to two Cu(II) ions in a bidentate and a monodentate fashion, respectively. The intra-cage $\text{Cu} \cdots \text{Cu}$ distance is 7.968(2) Å. Its packing structure is in the linear double-decker– $\cdots \text{SiF}_6^{2-}$ mode (Fig. S5†). The crystal structure of $[(\text{SiF}_6)@\text{Zn}_2\text{L}^2_4](\text{SiF}_6) \cdot 2\text{C}_4\text{H}_8\text{O} \cdot 4\text{CH}_2\text{Cl}_2$ is a typical Zn_2L_4 cage, as depicted in Fig. 2, and the coordination geometry of the Zn(II) ion is an octahedral arrangement with two SiF_6^{2-} groups in the *trans* position ($\text{Zn}-\text{F} = 2.095(5) - 2.273(5)$ Å; $\text{F}-\text{Zn}-\text{F}' = 180.0(0)$ °) and four pyridine N donors of four L^2 's on the basal

plane. Each L connects two zinc(II) ions in a bidentate mode with a free pyridyl donor. Concomitantly, for the nested SiF_6^{2-} , the equatorial Si–F bond lengths (1.637(4) Å) are slightly shorter than the axial Si–F lengths (1.733(5) – 1.746(6) Å). The intra-cage $\text{Zn} \cdots \text{Zn}$ distance is 8.113(2) Å. Its packing structure is in the linear cage– $\cdots \text{SiF}_6^{2-} \cdots \text{cage} \cdots \text{SiF}_6^{2-}$ mode (Fig. S5†). The solvate molecules of $[(\text{SiF}_6)_2@\text{Cu}_3\text{L}^1_4](\text{SiF}_6) \cdot 16\text{CH}_3\text{OH}$ were squeezed. The volumes of solvate molecules in $[(\text{SiF}_6)_2@\text{Cu}_3\text{L}^1_4](\text{SiF}_6) \cdot 16\text{CH}_3\text{OH}$ and $[(\text{SiF}_6)@\text{Zn}_2\text{L}^2_4](\text{SiF}_6) \cdot 2\text{C}_4\text{H}_8\text{O} \cdot 4\text{CH}_2\text{Cl}_2$ were 56.2% (10 282 Å³/18 304 Å³) and 37.8% (2093.4 Å³/5539.5 Å³), respectively, on the basis of a PLATON/SOLV calculation.⁵⁴

Discussion

Formation of SiF_6^{2-} during self-assembly of more than 2 weeks' duration requires some explanation, because the anion was not added to the self-assembly solution in a glass vessel. It should

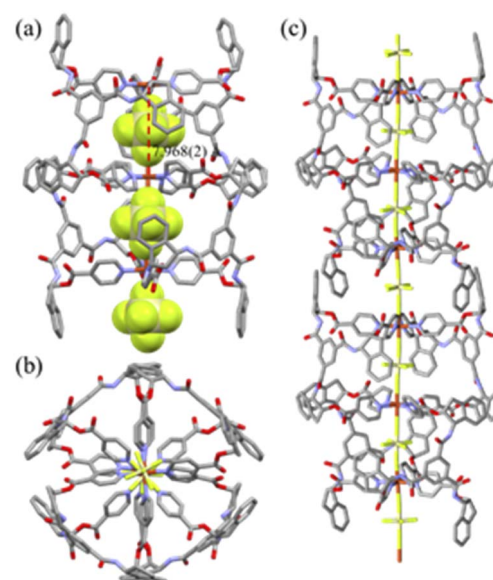


Fig. 1 Side view (a), top view (b), and packing structure (c) of double-decker, $[(\text{SiF}_6)_2@\text{Cu}_3\text{L}^1_4](\text{SiF}_6) \cdot 16\text{CH}_3\text{OH}$. The nested and outside bridged SiF_6^{2-} anions were clearly depicted in light green color.



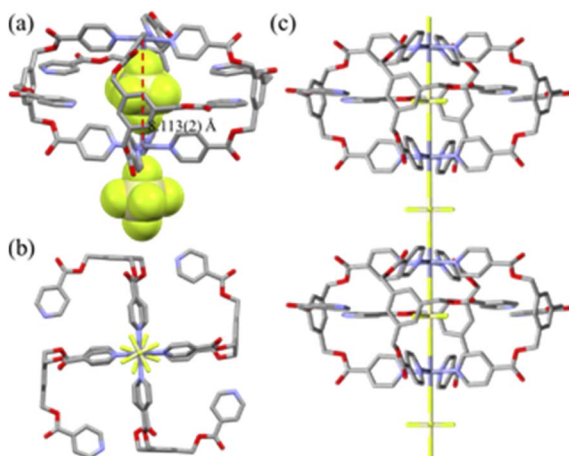
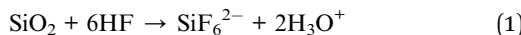


Fig. 2 Partial crystal structures of $[\text{Ag}(\text{s},\text{r}-\text{L})](\text{PF}_6) \cdot 3\text{C}_4\text{H}_8\text{O}_2 \cdot 0.5\text{H}_2\text{O}$ (a) and $[\text{Ag}(\text{r},\text{s}-\text{L})](\text{PF}_6) \cdot 3\text{C}_4\text{H}_8\text{O}_2 \cdot 0.5\text{H}_2\text{O}$ (b). The solvate molecules were omitted for clarity.

be noted that the SiF_6^{2-} anion replaces the starting BF_4^- anion in the self-assembly reaction and that it is formed after extracting Si^{4+} from the glass vessel in methanol solvent—a rare but well-known phenomenon.⁵⁵ The generation of SiF_6^{2-} by slow release of Si^{4+} from the glass vessel in the methanol solution was clearly confirmed, and the resultant anions were separated as counteranions. The SiF_6^{2-} anions appear to play significant roles as both encapsulator and bridge in the construction of the cage skeleton. The stable anion, by contrast, forms as a consequence of the hydrolysis of the BF_4^- anion and subsequent reaction of F^- with the Si–O moieties of the glass vessel^{56,57} in which a methanol solution of $\text{M}(\text{BF}_4)_2$ is kept for self-assembly or crystallization. The formation of SiF_6^{2-} seems to be promoted by the presence of a small quantity of H_2O in addition to a mixture solvent including methanol. Formation of SiF_6^{2-} from BF_4^- and PF_6^- in a glass vessel in water has been observed by other groups,^{30–32,56} but that of SiF_6^{2-} from SbF_6^- heretofore has not been recorded. The present self-assembly of MX_2 ($\text{M}^{2+} = \text{Cu}^{2+}, \text{Zn}^{2+}; \text{X}^- = \text{BF}_4^-, \text{PF}_6^-, \text{SbF}_6^-$) with each tridentate ligand in each glass vessel systematically transformed BF_4^- , PF_6^- or SbF_6^- into the SiF_6^{2-} anion according to the following eqn (1):



Of course, formation of SiF_6^{2-} from CF_3SO_3^- (C–F compound) could not be carried out in a similar reaction performed in a polypropylene vessel instead of a glass one; that is, the reaction did not yield crystals containing the SiF_6^{2-} anion.

The presence of SiF_6^{2-} in $\text{Me}_2\text{SO}-d^6$ was confirmed by ^{19}F NMR spectra (Fig. S6†). The SiF_6^{2-} occurred as a singlet at $\delta = -134$ ppm. Spectra taken of the sample preparation one month later indicated that almost all of the original BF_4^- anions had been converted to SiF_6^{2-} anions. As regards the formation of SiF_6^{2-} from PF_6^- and SbF_6^- anions, PF_6^- (-70.8 ppm) and SbF_6^- chemical shifts (-119.9 ppm) disappeared after 4 and 6 weeks, respectively, and appeared at the position of the SiF_6^{2-}

anion. As for construction of the coordination architecture, insight into the stability and geometry of a specific anion as a template is useful to the tuning of the shape and topology of coordination species. In the present study, the encapsulated and bridged SiF_6^{2-} anions helped to stabilize the crystal structure of the cages. Certainly, transformation of polyatomic anions and their role is a topic worthy of further investigation.

Conclusions

In summary, transformation of polyatomic anions BF_4^- , PF_6^- , and SbF_6^- into SiF_6^{2-} during self-assembly or recrystallization in a glass vessel was systematically confirmed. This shows that the surface of regular laboratory glassware should be given serious consideration for long-duration reactions or self-assembly with F^- species. Further studies on other means of anion-bridging or -encapsulation of cage units will contribute to the development of task-specific polyatomic anions for recognition as well as environmental molecular materials such as adsorbents and sensing materials.

Conflicts of interest

There are no conflicts to declare.

Acknowledgements

This work was supported by National Research Foundation of Korea (NRF) grants funded by the Korean Government [MEST] (2021R1A2C2005105, 2016R1A5A1009405 (OSJ)), and 2021R1I1A3059982 (YAL)). The X-ray crystallography at the PLS-II 2D-SCM beamline was supported in part by MSIP and POSTECH.

Notes and references

- 1 J. L. Anthony, J. L. Anderson, E. J. Maginn and J. F. Brennecke, *J. Phys. Chem. B*, 2005, **109**, 6366–6374.
- 2 Z. Wang, X. Li, W. Guo and Y. Fu, *Adv. Funct. Mater.*, 2021, **31**, 2009875.
- 3 J. P. Carpenter, C. T. McTernan, T. K. Ronson and J. R. Nitschke, *J. Am. Chem. Soc.*, 2019, **141**, 11409–11413.
- 4 P. A. Gale, R. Perez-Tomas and R. Quesada, *Acc. Chem. Res.*, 2013, **46**, 2801–2813.
- 5 D. H. Shin, M. Kim, Y. Kim, I. Jun, J. Jung, J. H. Nam, M. H. Cheng and M. G. Lee, *Pflugers Arch. - Eur. J. Physiol.*, 2020, **472**, 1003–1018.
- 6 Y. Zhao, Y. Li, S. Yuan, J. Zhu, S. Houtmeyers, J. Li, R. Dewil, C. Gao and B. Van der Bruggen, *J. Mater. Chem. A*, 2019, **7**, 6348–6356.
- 7 Y. Zhao, Y. Cotelle, L. Liu, J. López-Andarias, A.-B. Bornhof, M. Akamatsu, N. Sakai and S. Matile, *Acc. Chem. Res.*, 2018, **51**, 2255–2263.
- 8 Y. Bando, Y. Haketa, T. Sakurai, W. Matsuda, S. Seki, H. Takaya and H. Maeda, *Chem. Eur. J.*, 2016, **22**, 7843–7850.
- 9 S. Patnaik, D. P. Sahoo and K. Parida, *Carbon*, 2021, **172**, 682–711.

10 Y. Kim, P. Kang, Y. Jeon, H. M. Cho and M.-G. Choi, *Bull. Korean Chem. Soc.*, 2021, **42**, 240–244.

11 D. H. Sohn, T. Ohn, E. Han, A. B. Atar, S. J. Cho and J. Kang, *Bull. Korean Chem. Soc.*, 2021, **42**, 193–199.

12 J. Lee, Y. Hong, S. Yeon, D. Moon and T.-S. You, *Bull. Korean Chem. Soc.*, 2021, **42**, 563–566.

13 Z. Xu, X. Chen, R. Chen, X. Li and H. Zhu, *Npj Comput. Mater.*, 2020, **6**, 1–8.

14 D. Liu, J. Wang, Y. Wang and Y. Zhu, *Catal. Sci. Technol.*, 2018, **8**, 3278–3285.

15 J.-J. Liu, S.-B. Xia, Y.-L. Duan, T. Liu, F.-X. Cheng and C.-K. Sun, *Polymers*, 2018, **10**, 165.

16 G.-B. Li, Z. Zhang, L.-S. Liao, R.-K. Pan and S.-G. Liu, *Spectrochim. Acta, Part A*, 2021, **254**, 119588.

17 A. Caballero, F. Zapata and P. D. Beer, *Coord. Chem. Rev.*, 2013, **257**, 2434–2455.

18 J. E. Wong, H. Zastrow, W. Jaeger and R. von Klitzing, *Langmuir*, 2009, **25**, 14061–14070.

19 X. He, K. Zhang, Y. Liu, F. Wu, P. Yu and L. Mao, *Angew. chem.*, 2018, **130**, 4680–4683.

20 G. Sarada, A. Kim, D. Kim and O.-S. Jung, *Dalton Trans.*, 2020, **49**, 6183–6190.

21 J. Lee, S. Lim, D. Kim, O.-S. Jung and Y.-A. Lee, *Dalton Trans.*, 2020, **49**, 15002–15008.

22 S.-i. Noro and T. Nakamura, *NPG Asia Mater.*, 2017, **9**, e433.

23 M. Takeuchi, N. Matubayasi, Y. Kameda, B. Minofar, S.-i. Ishiguro and Y. Umebayashi, *J. Phys. Chem. B*, 2012, **116**, 6476–6487.

24 A. Pramanik, D. R. Powell, B. M. Wong and M. A. Hossain, *Inorg. Chem.*, 2012, **51**, 4274–4284.

25 D. Kim, G. Gwak, J. Han, D. Kim and O.-S. Jung, *Dalton Trans.*, 2022, **51**, 5810–5817.

26 J. Jaganathan, M. Sivapragasam and C. Wilfred, *J. Chem. Eng. Process Technol.*, 2016, **7**, 1–6.

27 R. P. Swatloski, J. D. Holbrey and R. D. Rogers, *Green Chem.*, 2003, **5**, 361–363.

28 C. A. Reed, *Chem. N. Z.*, 2011, **75**, 174–179.

29 T. H. Noh, H. Lee, Y.-A. Lee and O.-S. Jung, *Inorg. Chim. Acta*, 2013, **405**, 9–14.

30 M.-Y. Sun, X.-Z. Wang, Z.-Y. Chen, X.-P. Zhou and D. Li, *Inorg. Chem.*, 2019, **58**, 12501–12505.

31 M. Mizuhata, Y. Saito, M. Takee and S. Deki, *J. Ceram. Soc. Jpn.*, 2009, **117**, 335–339.

32 D. L. Reger, A. E. Pascui and M. D. Smith, *Eur. J. Inorg. Chem.*, 2012, **2012**, 4593–4604.

33 A. Galstyan, W. Z. Shen, E. Freisinger, H. Alkam, W. Hiller, P. J. Sanz Miguel, M. Schürmann and B. Lippert, *Chem. Eur. J.*, 2011, **17**, 10771–10780.

34 W. Chen, J. Chu, I. Mutikainen, J. Reedijk, U. Turpeinen and Y.-F. Song, *CrystEngComm*, 2011, **13**, 7299–7304.

35 M. M. Nielsen and C. M. Pedersen, *Chem. Sci.*, 2022.

36 E. Wiberg, A. F. Holleman and N. Wiberg, *Inorganic chemistry*, Academic press, 2001.

37 J. Frayret, A. Castetbon, G. Trouve and M. Potin-Gautier, *Chem. Phys. Lett.*, 2006, **427**, 356–364.

38 G. O. Bianchetti, C. L. Devlin and K. R. Seddon, *RSC Adv.*, 2015, **5**, 65365–65384.

39 E. Urbansky and M. Schock, *Int. J. Environ. Sci.*, 2000, **57**, 597–637.

40 H. Amouri, C. Desmarests and J. Moussa, *Chem. Rev.*, 2012, **112**, 2015–2041.

41 M. Shindo and T. Iwata, *Synlett*, 2022, **33**, 531–545.

42 C. M. Thompson, *Dianion chemistry in organic synthesis*, CRC press, 1994.

43 T. W. Hudnall, C.-W. Chiu and F. P. Gabbai, *Acc. Chem. Res.*, 2009, **42**, 388–397.

44 G. Derkson, P. Poon and A. Richardson, *J. Dent. Res.*, 1982, **61**, 660–664.

45 L. C. Chow, S. Takagi, C. M. Carey and B. Sieck, *J. Dent. Res.*, 2000, **79**, 991–995.

46 R. P. Sharma, R. Sharma, R. Bala, U. Rychlewska, B. Warzajtis and V. Ferretti, *J. Mol. Struct.*, 2005, **753**, 182–189.

47 J. Lusher and F. Sebba, *J. Appl. Chem.*, 1966, **16**, 129–132.

48 D. Kim, K.-D. Seo, Y.-B. Shim, K. Lee, S. H. Lee, Y.-A. Lee and O.-S. Jung, *Dalton Trans.*, 2022, **51**, 6046–6052.

49 D. Choi, H. Lee, J. J. Lee and O.-S. Jung, *Cryst. Growth Des.*, 2017, **17**, 6677–6683.

50 J. W. Shin, K. Eom and D. Moon, *J. Synchrotron Radiat.*, 2016, **23**, 369–373.

51 Z. Otwinowski and W. Minor, *Methods in Enzymology*, ed. C. W. Carter Jr. and R. M. Sweet, Academic Press, New York, 1997, 276, p. 307.

52 G. M. S. A. D. A. B. S. Sheldrick, *A program for Empirical Absorption Correction of Area Detector Data*, University of Göttingen, Germany, 1996.

53 G. M. Sheldrick, *Acta Crystallogr., Sect. C: Struct. Chem.*, 2015, **71**, 3–8.

54 A. Spek, *Acta Crystallogr., Sect. D: Biol. Crystallogr.*, 2009, **65**, 148–155.

55 B. O. Mysen and D. Virgo, *Chem. Geol.*, 1986, **57**, 303–331.

56 J. Y. Wu, M. S. Zhong and M. H. Chiang, *Chem. Eur. J.*, 2017, **23**, 15957–15965.

57 J. Jia, A. J. Blake, N. R. Champness, P. Hubberstey, C. Wilson and M. Schroder, *Inorg. Chem.*, 2008, **47**, 8652–8664.

